The Effects of Oil Entrained Air on the Dynamic Performance of a Hydraulically Driven Multibody System

Mohammadi Manouchehr, Kiani-Oshtorjani Mehran, Mikkola Aki

DOI: 10.15866/iremos.v13i4.18612

Praise Worthy Prize

This paper is available online at www.praiseworthyprize.org
International Review on Modelling and Simulations (I.RE.MO.S.), Vol. 13, N. 4
ISSN 1974-9821 *August 2020*

The Effects of Oil Entrained Air on the Dynamic Performance of a Hydraulically Driven Multibody System

Manouchehr Mohammadi, Mehran Kiani-Oshtorjani, Aki Mikkola

Abstract – *In co-simulation, a number of subsystems sharing details of a system, are coupled to exchange data. The subsystem level development of each package enhances the computational efficiency, and more sophisticated packages can be created. However, the data exchange is not always straight forward as different packages can be developed by different research or industrial centers. Therefore, some standards such as Functional Mock-up Interface (FMI) are developed to facilitate the data exchange in co-simulation or co-integration. In this work, the co-simulation approach is employed to investigate the effects of dissolved air on the dynamic performance of a hydraulically driven multibody system. To this end, the subsystems of multibody system dynamics and a hydraulic model are coupled by using the FMU procedure. The utilized FMUs are produced by using an XML model description and a C code for the hydraulic part. The multibody mechanism under investigation is a jib crane model containing three bodies. The model is studied by exciting different sine inputs having known frequencies while varying the amount of dissolved air in the hydraulic system. The results have illustrated that by increasing the amount of entrained air, the pressure amplitude decrease. In addition, the results demonstrated that the amount of the air does not have effects on shifting the system frequency.*

Keywords*: Bulk Modulus, Entrained Air, FMU, Hydraulic Circuit, Multibody System*

Nomenclature

A_A	Cylinder area
A_B	Piston area
$\mathbf{A}_i$	Rotation matrix of i^{th} body
$\mathbf{A}_i^j$	Relative rotation matrix for continuous i^{th} body and j^{th} body
$\mathbf{A}_j$	Rotation matrix of j^{th} body
A_t	Cross-sectional area of the valve
B_i	i^{th} rigid body
B_j	j^{th} rigid body
$\boldsymbol{C}$	Quadratic velocity vector
c	Constant related to the oil properties
C_d	Discharge coefficient
C_n	Corresponds to the variations of density of air
C_{pv}	Valve flow rate coefficient
D_i	Number of DOF for the i^{th} joint
$\mathbf{d}_i^j$	Relative displacement vector between j^{th} and i^{th}bodies
E	Point location of the joint
f	Frequency
F_s	Force generated by the cylinder
F_μ	Friction force
k	Constant stands for the process
l	Stroke length in its maximum value
$l_a, l_b, l_c, l_d, l_e, l_f, l_g, l_h, l_i, l_j$	Lengths for different parts of the jib-crane model
l_l	Length of the lift boom
l_p	Length of the pillar
l_t	Length of the tilt boom
$\mathbf{M}$	Mass matrix
m_l	Mass of lift boom
m_p	Mass of pillar
m_t	Mass of tilt boom
N_b	Number of bodies
N_f	Number of degrees of freedom
N_{f_b}	Number of relative degrees of freedom that considered from body N_b to the ground
P	Pressure
P_A, P_B	Pressure values
P_b	Number of joints in the path from body N_b to the ground
P_p	Pump operation pressure
P_1, P_2	Pressures of the throttle valve in its both sides
P_T	Tank operation pressure
$\mathbf{Q}$	Generalized external force vector
Q	Point location of the joint
Q_V	Volumetric flow rate
Q_{in}	Incoming flow rate
Q_{out}	Outgoing flow rate
Q_t	Volumetric turbulent flow rate
$\dot{\mathbf{q}}$	Generalized velocity vector
$\mathbf{R}$	Velocity transformation matrix

Available online by August 31st, 2020 https://doi.org/10.15866/iremos.v13i4.18612

$\mathbf{R}_{N_b}$	Rows of the matrix **R**
$\mathbf{r}_i$	Global position vector of a point on i^{th} body
$\mathbf{r}_j$	Global position vector of a point on j^{th} body
$\mathbf{s}_i$	Rotated position vector of a point on i^{th} body with respect to the rotation matrix
$\bar{\mathbf{s}}_i$	Position vector of a point on i^{th} body within its body reference coordinate system
t	Time
U	Spool position
U_{in}	Control signal
V	Volume
V_{in}	Incoming hydraulic cylinder volume
V_{out}	Outgoing hydraulic cylinder volume
x	Piston position at each time step
$\dot{\mathbf{z}}$	Relative joint velocity vector
γ	Constant stands for the process
δ_d	Corresponds to the variations of density of air
θ	Implicitly defines the air volume fraction
ρ	Fluid density
β	The effective bulk modulus
ρ_l	Oil density
τ_v	Relaxation time
$\boldsymbol{\omega}_i$	Global angular velocity of i^{th} body
$\tilde{\boldsymbol{\omega}}_i$	Skew-symmetric matrix of the global angular velocity of i^{th} body
$\boldsymbol{\omega}_i^j$	Relative angular velocity between i^{th} and j^{th} bodies
$\boldsymbol{\omega}_j$	Global angular velocity of j^{th} body
Abbreviations	
avf	Air volume fraction
Amp	Amplitude
DOF	Degrees of Freedom
FMI	Functional Mock-up Interface
FMU	Functional Mock-up Unit
HLA	High-Level Architecture
MPI	Message Passing Interface
XML	Extensible markup language

I. Introduction

In the application of mobile machines, power density is typically a critical design aspect. For this reason, mobile machines consist of mechanisms actuated by hydraulic power systems. Accordingly, in machine designing, it is important to analyze the coupled dynamic behavior of mechanical and hydraulic systems.

Hydraulically driven mechanical systems can be analyzed by employing a combination of multibody system dynamics and lumped fluid theory. The multibody system often takes a larger time step in comparison with lumped fluid theory due to high numerical stiffness associated with the computation of hydraulics [1]. The high stiffness of hydraulics can be due to the presence of small volumes in the circuit in which their saturation time is smaller than one integration time step. These small volumes can be found in closed valves or at the end stroke of pistons. Kiani-Oshtorjani et al. [2] have introduced a perturbed model to overcome the numerical difficulty associated with a small volume in the hydraulic circuit. Accordingly, they proposed the use of an algebraic equation instead of a non-linear differential equation for modelling the small volumes. By doing so, they have succeeded in increasing the integration time by one order of magnitude. This model is successfully implemented by Rahikainen et al. [3] for a four-bar mechanism actuated with a hydraulic system. In addition to a small volume, the precise modelling of an effective bulk modulus can also alleviate the problems associated with the numerical instabilities of hydraulic simulations.

This is simply because the bulk modulus is directly related to the stiffness of the hydraulic actuators. Many scholars have studied the formulation of the effective bulk modulus and evaluated the effect of entrained air in the fluid while increasing the pressure, as presented in the literature [4]-[11]. Higher and unrealistic values for the bulk modulus can lead to high frequency fluctuations in the system, and consequently, a smaller integration time step is needed. There are number of studies on coupling multibody system dynamics and the hydraulic circuit systems; specifically, many studies examine oscillation reduction and the optimal vibration damping in multibody system dynamics coupled with a hydraulic system [12]-[14]. A number of researchers have studied the improvement of a tuned vibration absorber and other techniques to reduce structural and control the vibrations [15]-[20]. In addition, several scholars have also studied on controlling the stiffness, damping characteristics, and flow stability that is induced by fluids [21]- [23]. Yuming Yin et al. have studied a hydro-pneumatic suspension system utilizing gas and oil. They used a suspension system with emulsion gas-oil and noticed that the entrapped gas in the system can remarkably influence the effective stiffness and damping properties [13].

Furthermore, a number of studies have been done on dampers' design to create frictions in the joints between the bodies, generating shear force on rigid bodies by using fluids [24], [25]. It is well-known that the effective bulk modulus is directly influenced by the amount of entrained air [26]. Furthermore, the amount of the entrapped gas in the suspension system and the amount of entrained air (not the dissolved air [27] in the oil can affect the oil properties- especially the bulk modulus [28]. In the hydraulic circuit system, Yu et al. have considered the level of the entrained air in the fluid by evaluating 'the air bubble variation coefficient' and 'the ratio of specific heat for air'. They considered two values of the air bubble variation coefficient in the fluid. By increasing the pressure, the bulk modulus values decreased for the oil with greater air bubble variation coefficients [7], [26]. The aim of this study is to provide an understanding about the effects of the bulk modulus

on the dynamic performance of a multibody system. To this end, the amount of entrained air within the description of the bulk modulus is varied and analyzed.

In this study, a mechanical system and hydraulics are solved using the C/C++ programming language. The FMU is used as an interface to transfer hydraulic data to the mechanical code. FMU is, in fact, the composition of the XML model description and a code written in C to solve the hydraulic circuit. In addition, Matlab-Simulink is used to provide the inputs for the hydraulics. The hydraulic circuit system is defined as containing two cylinder-pistons. The results will show that by increasing the amount of the entrained air in the oil, the oscillation/damping behavior of the system can be affected.

The rest of the paper is organized as follows. Section II explains, the method, extracting the equations of motion for the multibody system and the hydraulic part.

Section III introduces the numerical example. Section IV-results and discussion-details the differences in the results of the hydraulic system with different entrained air in the oil. The section also addresses the hydraulic system modelling used in the studied case. Conclusions are presented in the final section.

II. Methods

This section describes the equations of motion based on the semi-recursive multibody systems. Subsequently, the hydraulic formulation is expressed for hydraulic circuit systems which have interconnections with multibody systems.

II.1. Equations of Motion

In this section, equations of motion based on a semi-recursive multibody approach are briefly reviewed. For each body, translational and rotational generalized coordinates are used to describe the system kinematics.

These coordinates will be then transferred to relative joint coordinates to enhance computational efficiency [29]. A multibody system with N_b number of bodies, connected by kinematic constraints, bodies B_i and B_j with respect to the fixed frame O (Figure 1) are considered.

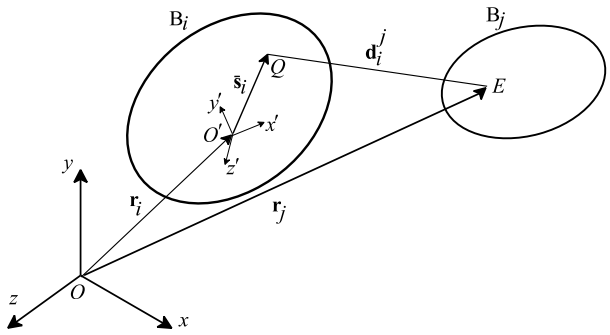

Fig. 1. Two contiguous bodies

Points Q and E in Fig. 1 are the joints' positions on body B_i and body B_j, respectively. The joint relative displacement vector between two points Q and E is denoted by $\mathbf{d}_i^j$. The position $\mathbf{r}_j$ at point E in the reference frame O can be written as:

$$\mathbf{r}_j = \mathbf{r}_i + \mathbf{A}_i\bar{\mathbf{s}}_i + \mathbf{d}_i^j \tag{1}$$

where $\mathbf{r}_i$ is the position vector for the reference frame of body B_i with respect to the global coordinate, $\mathbf{A}_i$ is the rotation matrix of body B_i, $\bar{\mathbf{s}}_i$ is the location of Q in the reference frame of the body B_i. The body B_j rotation matrix can be expressed as:

$$\mathbf{A}_j = \mathbf{A}_i\mathbf{A}_i^j \tag{2}$$

where $\mathbf{A}_i^j$ is the relative rotation matrix for continuous body B_i and body B_j. Correspondingly, the expression's velocities of point E can be written as:

$$\dot{\mathbf{r}}_j = \dot{\mathbf{r}}_i + \tilde{\boldsymbol{\omega}}_i\mathbf{s}_i + \dot{\mathbf{d}}_i^j \tag{3}$$

$$\boldsymbol{\omega}_j = \boldsymbol{\omega}_i + \boldsymbol{\omega}_i^j \tag{4}$$

where $\dot{\mathbf{r}}_j$, $\dot{\mathbf{r}}_i$, and $\dot{\mathbf{d}}_i^j$, are the time derivatives of $\mathbf{r}_j$, $\mathbf{r}_i$ and $\mathbf{d}_i^j$, respectively. In equation (3), $\tilde{\boldsymbol{\omega}}_i$ is a 3×3 skew-symmetric matrix, and $\mathbf{s}_i = \mathbf{A}_i\bar{\mathbf{s}}_i$. In equation (4), $\boldsymbol{\omega}_j$ and $\boldsymbol{\omega}_i$ are the angular velocities for bodies B_j and B_i, respectively, and $\boldsymbol{\omega}_i^j$ is the relative angular velocity between body B_i and body B_j. Using the kinematics shown above and by employing the concept of virtual work, equations of motion can be written as [30]:

$$\delta\dot{\mathbf{q}}^{\mathrm{T}}(\mathbf{M}\ddot{\mathbf{q}} + \mathbf{C} - \mathbf{Q}) = 0 \tag{5}$$

where $\delta\dot{\mathbf{q}}$ are the virtual velocities of generalized coordinates of dimension $6N_b$, $\mathbf{M}$ is the diagonal mass matrix, $\ddot{\mathbf{q}} = \{\ddot{\mathbf{q}}_1^{\mathrm{T}}\ddot{\mathbf{q}}_2^{\mathrm{T}}\dots\ddot{\mathbf{q}}_{N_b}^{\mathrm{T}}\}^{\mathrm{T}}$, $\mathbf{C} = \{\mathbf{C}_1^{\mathrm{T}}\mathbf{C}_2^{\mathrm{T}}\dots\mathbf{C}_{N_b}^{\mathrm{T}}\}^{\mathrm{T}}$, quadratic velocity vector, and $\mathbf{Q} = \{\mathbf{Q}_1^{\mathrm{T}}\mathbf{Q}_2^{\mathrm{T}}\dots\mathbf{Q}_{N_b}^{\mathrm{T}}\}^{\mathrm{T}}$, external forces and torques, are vectors of dimension $6N_b$. The terms in parenthesis in equation 5 express the Newton-Euler equation [30]. The term $\delta\dot{\mathbf{q}}$ must satisfy the kinematic constraints, i.e. it should be kinematically admissible. The virtual velocity vector $\delta\dot{\mathbf{q}}$ of dimension $6N_b$ can be defined in terms of vector $\delta\dot{\mathbf{z}}$ of the dimension N_f, where N_f is the number of degrees of freedom (DOF) of the system, and $\delta\dot{\mathbf{z}}$ are the virtual velocities of the joint coordinates. The velocity transformation matrix, $\mathbf{R}$, which relates the definition of the relative joint coordinates to the generalized coordinates, as below:

$$\dot{\mathbf{q}} = \mathbf{R}\dot{\mathbf{z}} \tag{6}$$

where $\dot{\mathbf{q}}$ is the generalized velocity vector, and $\dot{\mathbf{z}}$ is the joint velocity vector. Equation (6) is valid when the

constraints are time independent. The acceleration of generalized coordinates can be obtained by taking derivatives of equation (6) with respect to time:

$$\ddot{\mathbf{q}} = \mathbf{R}\ddot{\mathbf{z}} + \dot{\mathbf{R}}\dot{\mathbf{z}} \tag{7}$$

By using equations (6) and (7), equation (5) can be written as:

$$\delta\dot{\mathbf{z}}^{\mathrm{T}}\mathbf{R}^{\mathrm{T}}\left[\mathbf{M}\left(\mathbf{R}\ddot{\mathbf{z}} + \dot{\mathbf{R}}\dot{\mathbf{z}}\right) + \mathbf{C} - \mathbf{Q}\right] = \mathbf{0} \tag{8}$$

Equation (8) for any virtual velocity $\delta\dot{\mathbf{z}}^{\mathrm{T}}$ is actual, and the virtual velocities can be eliminated. Therefore, the equation of motion can be written as:

$$\mathbf{R}^{\mathrm{T}}\mathbf{M}\mathbf{R}\ddot{\mathbf{z}} = \mathbf{R}^{\mathrm{T}}(\mathbf{Q} - \mathbf{C}) - \mathbf{R}^{\mathrm{T}}\mathbf{M}\dot{\mathbf{R}}\dot{\mathbf{z}} \tag{9}$$

which expresses the N_f number of ordinary differential equations of motion with respect to relative joint coordinates. Note that, the rows of the matrix **R** are expressed in $\mathbf{R}_{N_b}$ when the zero columns are terminated.

The matrix $\mathbf{R}_{N_b}$ has the size of $(6 \times N_{f_b})$ where N_{f_b} is the number of relative degrees of freedom that *are* considered from body N_b to the ground [30]. Matrix $\mathbf{R}_{N_b}$ is illustrated as:

$$\mathbf{R}_{N_b} = \left[\mathbf{R}^1_{N_b}\mathbf{R}^2_{N_b}\mathbf{R}^3_{N_b}\dots\mathbf{R}^{P_b}_{N_b}\right] \tag{10}$$

where P_b is the number of joints in the path from body N_b to the ground. The size for each submatrix $\mathbf{R}^i_{N_b}$ is $6 \times D_i$, where D_i is the number of DOF for the joint *i*. The term $\mathbf{R}^i_{N_b}$ is expressed in the literature for different joint types [30]. By using cut-joint, closed-loop systems can be changed to open-loop ones [31], [32]. The equations of motion for a closed-loop system, which is converted to an open-loop *system* are presented by Avello et al. [30].

II.2. Hydraulic Modeling

This section starts with describing the lumped fluid theory to model the hydraulic circuit system and continues to elaborat*e* on the hydraulic parameters affecting the simulation time step.

Lumped Fluid Theory: in this study, the hydraulic equations are formed by implementing the lumped fluid theory. In this method, the hydraulic circuit is modeled by assuming evenly distributed pressures in distinguished volumes.

Differential equations are considered for the volumes in which the pressures are solved. In this case, the volumes are set apart from each other using a throttling that the fluid will flow through. Furthermore, the throttles are used in substitute for flow control valves, pressure valves, and the pipelines that are used in real systems. According to the lumped fluid theory, the pressure in the volume of the hydraulic circuit can be calculated using a differential equation as follows [33]:

$$\frac{dP}{dt} = \frac{\beta}{V}\left(Q_{in} - Q_{out} - \frac{dV}{dt}\right) \tag{11}$$

where P is the pressure, β is the effective bulk modulus, V is the volume, Q_{in} is the incoming flow rate and Q_{out} is the outgoing flow rates, and $\frac{dV}{dt}$ is the volume V changing with respect to time. The container flexibility and the dissolved air *e*ffects are taken into account in the fluid bulk modulus, by definition of the effective bulk modulus [27]. Moreover, the explanation of the volumetric turbulent flow rate Q_t is as follow*s* [34]:

$$Q_t = C_d A_t \sqrt{\frac{2(P_2 - P_1)}{\rho}} \tag{12}$$

where C_d is the discharge coefficient, A_t is the cross-sectional area of the valve, P_1 and P_2 are pressures of the throttle valve on both its sides, and ρ is the fluid density.

The semi-empirical method is utilized in this study, to explain the volumetric flow rate that means that the valve's parameters are derived via measurements [35].

Generally, the dimension*s* and the input pressures can be used to model a hydraulic cylinder. The hydraulic cylinder volume can be written as follows:

$$V_{in} = xA_A \tag{13-a}$$

$$V_{out} = (l - x)\,A_B \tag{13-b}$$

where A_A and A_B are the areas of the piston*'s* front side, and the piston rod*'s* side surfaces, respectively, l is the stroke length in its maximum value, and x is the piston position at each time. The piston motions create the volumetric flow rate that can be shown as:

$$Q_{in} = \dot{x}A_A \tag{14}$$

$$Q_{out} = -\dot{x}A_B \tag{15}$$

The force F_s, which is generated by the cylinder, can be formed as:

$$F_s = P_A A_A - P_B A_B - F_\mu \tag{16}$$

where F_μ is the friction force, and P_A and P_B are the pressure values.

The spool position of the valve, U, describes the valve behavior and can be written for magnetically actuated valves by using a first-order differential equation:

$$\dot{U} = \frac{U_{in} - U}{\tau_v} \tag{17}$$

where U_{in} is the control signal, and τ_v is the relaxation time of the valve.

The flow rate in the system is related to the spool position of the valve, which can be written as:

$$Q_V = 2Uc\sqrt{\Delta P} \tag{18}$$

where Q_V is the volumetric flow rate and c is the constant, related to the oil properties. The effective bulk modulus: The simulation of complex systems combining the mechanical and hydraulic parts usually takes smaller time steps compared to pure mechanical ones. A number of parameters affect the hydraulic stiffness, which cause the mechanical system response [36], including the presence of a small volume in the circuit and the value of the bulk modulus. The small volume of hydraulic components divided into a large bulk modulus value makes a very small parameter multiplied with the largest order of differential equations, and consequently makes the equation numerically singular. On the other hand, to shed more light on the effects of the hydraulic oil's bulk modulus accuracy on the stiffness of hydraulic systems, this study employs a thermodynamics-based model for the bulk modulus taking into account both the air compression and the dissolution processes. The oil bulk modulus relation relies on the fact that the air can be either dissolved into the hydraulic oil or entrained as bubbles. Whereas the amount of entrained air significantly changes the value of the bulk modulus, the dissolved air does not have an important effect on it. As a result, considering the dissolution process occurring at the rate of θ, the proposed relation can be expressed as:

$$\beta = \frac{k\gamma\delta_d V P^{\frac{1}{k}+1}}{C_n\left(\delta_d + \frac{\gamma P^{\frac{1}{k}}\theta}{\rho_l} + \frac{k\gamma\theta P^{\frac{1}{k}+1}}{C_n\rho_l}\delta_d\right)} \tag{19}$$

where, k and γ stand for the process, C_n and δ_d correspond to the variations of density of air, and ρ_l is the oil density. In equation 19, γ and θ implicitly define the air volume fraction, (avf), in the hydraulic system formulas.

The compressibility of the oil can change the time scale of the system. In other words, the non-compressible oil yields a very small time scale for the hydraulic components and consequently makes the system singular (singularity usually occurs in a system with very small time scales).

The compressible oil can increase the time in which the system responds (time scale) and can conduct to larger integration time steps. In reality, the hydraulic oil to some extent contains entrained air.

Therefore, the simulation of hydraulic circuits in which the oil compressibility is considered may increase the integration time step. The external force acting on the cylinder from the mechanical part causes the hydraulic oil to be compressed, and as a result, to have a higher bulk modulus value. In addition, the frequency at which the load is imposed can effectively change the behavior of the system. Moreover, the amount of entrained air in the oil has a significant influence on the compressibility of the oil and consequently on the simulation time.

II.3. Procedure

The analysis of the complexity of a mobile machine typically requires converting a sophisticated system to simpler components having proper interactions. These components, which work in different domains such as mechanics and hydraulics, can be coupled [37] using a co-simulation procedure for instances [1], [38], [39]. In the co-simulation approach, a divided system can be simulated using parallelization approaches such as openMP or MPI. Despite some disadvantages, such as being time-consuming in some applications [40], or increasing coupling errors [41], the co-simulation is an effective approach for collecting information from the subsystems to enhance the communications among them [42]. One of the recently developed tools facilitating model exchange and multi-physics co-simulations is the concept of the Functional Mock-up Interface (FMI). The FMI standard provides the users with the ability to combine their models within a package Functional Mock-up Unit (FMU). An FMU, in turn, refers to the interaction between the XML files and the C code [43], [44]. This model is under development by Modelica Association [45]. Another alternative to the FMI standard is High-Level Architecture (HLA) [46] for complex systems where several simulations should be combined.

In this study, FMU packages for a hydraulic system are created. Each FMU package possesses different oil properties. These packages, in fact, control the hydraulic circuit response by manipulating the oil bulk modulus values. The variation in the bulk modulus values is obtained by manipulating the amount of entrained air in the oil. The hydraulic circuit is modeled using the C/C++ code written as an FMU and combined with the multibody formulation as an interface. A number of input files are provided to excite the model.

III. Numerical Example

The case under investigation is a jib crane, which is modeled using the multibody approach (Fig. 2). As stated earlier, the model is divided into two subsystems, mechanical and hydraulics, which interact with each other. The fourth order Runge-Kutta is used as a time integration procedure. In this study, the oil properties are manipulated to investigate the oil effects on the mechanical system. The mechanical parameters of the jib crane are shown in Table I, where m_p, m_l and m_t are the masses for the pillar, the lift boom and the tilt boom, respectively.

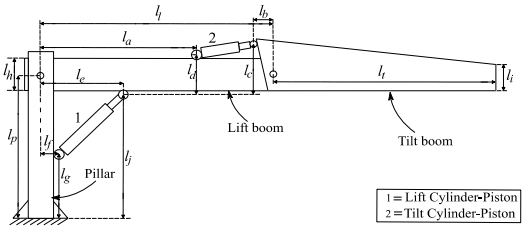

Fig. 2. A schematic of the jib crane model

TABLE I
MECHANICAL PARAMETERS FOR THE JIB CRANE

Parameter	Unit	Value
l_p	m	1.52
l_l	m	2.32
l_t	m	2
l_a	m	1.3
l_b	m	0.18
l_c	m	0.48
l_d	m	0.32
l_e	m	0.8
l_f	m	0.37
l_g	m	0.32
l_h	m	0.3
l_i	m	0.15
l_j	m	1.44
m_p	kg	135
m_l	kg	270
m_t	kg	114

Fig. 3 displays the hydraulic circuit schematic of the system under investigation. The circuit consists of two actuators controlled by valves connected to the pump and the tank. Table II shows the operating pressures and other hydraulic parameters.

IV. Results and Discussion

In this section the effects of the dissolved air on the multibody damping characteristics is examined. To this end, a hydraulic oil containing various amounts of entrained air is selected. By considering the amount of entrained air in the hydraulic oil, the bulk modulus value consequently changes/adapts.

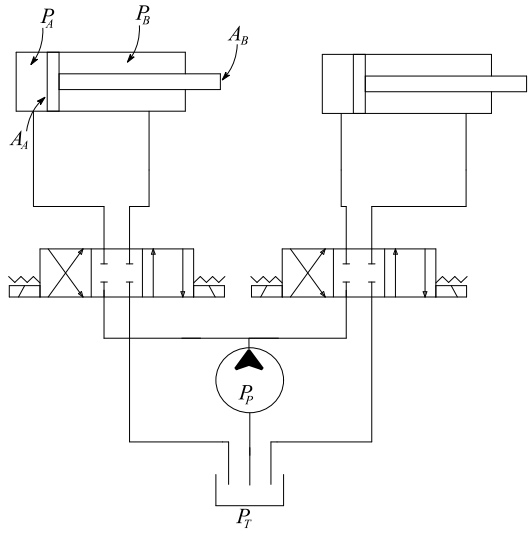

Fig. 3. The schematic of the hydraulic circuit for the case study

TABLE II
HYDRAULIC PARAMETERS FOR THE JIB CRANE

Parameter (Unit)	Description	Value
τ_v (s)	Relaxation time	0.1
C_{pv} (s)	Valve flow rate coefficient	3.984×10^{-8}
P_p (Pa)	Pump operation pressure	80×10^5
P_T (Pa)	Tank operation pressure	1×10^5
A_A (m^2)	Cylinder area	1.963×10^{-3}
A_B (m^2)	Piston area	0.314×10^{-3}

In this study, it is assumed that the oil characteristics remain the same for all scenarios, and the only parameter changing is the air volume fraction. To study the variation of the bulk modulus versus pressure change, based on the proposed relation, an arbitrary point is required on the *P-β* diagram for the oil. Therefore, three scenarios corresponding to three arbitrary points are selected and presented in Table III. The input files for the real-time software are provided with Matlab-Simulink.

The input files generate the signal corresponding to the valve position. This signal can be a real number between 10 and -10 related to a fully open or fully closed valve. For the results, two different input scenarios signals are generated for this case study: the step signal and the sine signal (Figures 4(a) and 4(b), respectively).

The input files are generated for the sine function at different frequencies. The integration time steps for both the real-time simulation software and Simulink have been set to 10^{-3} seconds. Figure 5 shows the frequency response (frequency (*f*) versus the amplitude (*Amp*)) of pressure signals for the air volume fraction of 1.9 and the input excitation frequency of 5 Hz. As this Figure shows, a peak occurs at the same frequency as the given input.

The other peaks in the Figure are caused by multibody mechanisms and have been observed in all the simulations.

TABLE III
THREE EMPLOYED AIR VOLUME AND THEIR CORRESPONDING PRESSURES AND BULK MODULUS VALUES

Air Volume Fraction (avf)	*P* (Pa)	*β* (Pa)
0.19	65.168×10^5	20905×10^5
0.345	65.116×10^5	16352×10^5
0.44	65.271×10^5	16959×10^5

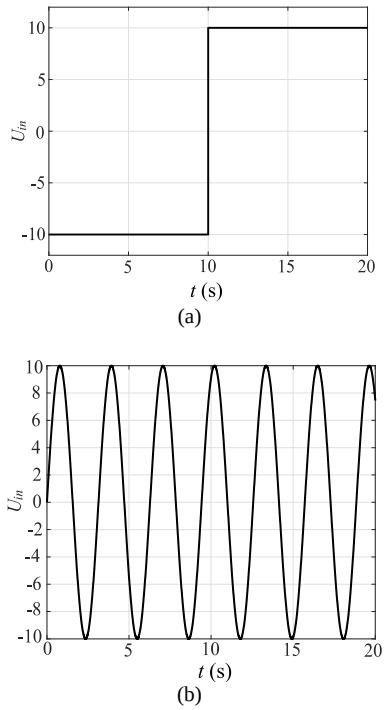

Figs. 4. Two input signals used in this case study; (a) step signal. b sine signal

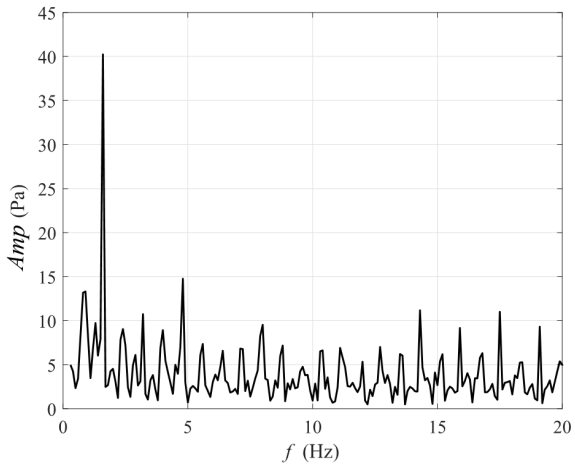

Fig. 5. Frequency versus the pressure amplitude at air volume fraction 1.9 and frequency 5 Hz

A number of parameters affect the dynamic response of the system, such as external forces, friction, hydraulic oil properties, system length, time characteristics, constraint and initial conditions. Among them, the damping of the system due to the manipulation of hydraulic oil properties is the factor that has been changed in the study. Even though the input external force is the reason for exciting all the system frequencies, the effect of the input itself can be seen at the same frequency as the input. However, this manipulation of hydraulic oil stiffness might also shift the frequency response even though the input force frequency remains fixed. Therefore, the first investigation is to measure the damping of two systems with different oil stiffnesses.

Figure 6 plots the pressure response of the lift cylinder versus time. The input signal for this study is a step function (Figure 4(a)). Table IV depicts the values for D_1, D_2, and $\frac{D_1}{D_2}$.

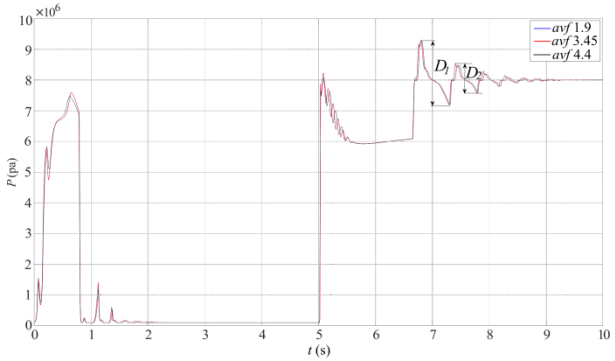

Fig. 6. Pressure response of the lift cylinder versus time excited by a step input

TABLE IV
THE RESULTS OF THE MODEL EXCITED BY A STEP INPUT

---	avf=1.9	avf=3.45	avf=4.4
D_1	20.98×10^5	21.13×10^5	21.01×10^5
D_2	9.54×10^5	9.80×10^5	8.94×10^5
$\frac{D_1}{D_2}$	2.1992	2.1561	2.3501

As a result, the pressure signal oscillates slightly before reaching its steady-state condition. In Fig. 6, the ratio of oscillation amplitudes $\frac{D_1}{D_2}$ corresponds to the damping of the system (the higher the ratio, the more the oscillations, the lesser the damping). Figure 6 reveals that the pressure response relies on the step function in all three scenarios, showing that all systems have the same damping features. As a result, the system's frequency response to the input signal does not shift due to the damping. Another conclusion is that the amount of air has no effect on the damping of the system. Figure 7 is prepared by feeding different *sine* functions with the same amplitude of 10 and different frequencies.

Therefore, the x-axis of the figure stands for the frequencies fed as an input to the system. Thus, the y axis is the amplitude of the pressure signal (*Amp*) (output) at the same frequency (with a very small tolerance). The effects of the input are expected to appear without any shifting in the pressure frequency response, as the damping of all systems is the same. This figure shows that a smaller amount of air yields higher amplitudes for all inputs (frequencies), and vice versa. Furthermore, the moderate air volume fraction of 3.45 moves between two other scenarios with air volume fractions of 1.9 and 4.4.

In addition, there is a local minimum at some frequencies, e.g., the frequency of 3 Hz, meaning that it is possible to set an input with lesser importance to the pressure response. It appears that after the frequency of 4 Hz, the amplitude does not significantly depend on the input frequency and only oscillates around a constant value. However, the effects of air are more obvious in that region in comparison to the lower frequencies below 2 Hz where the amplitudes rely on each other.

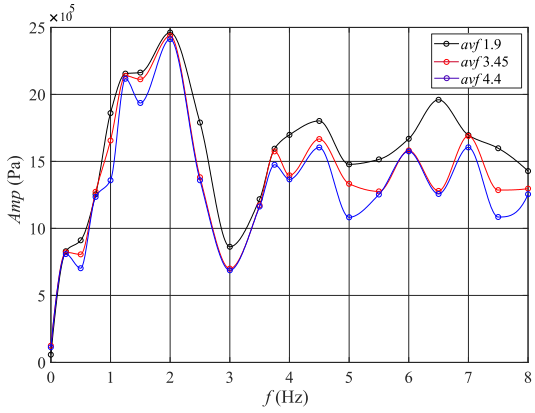

Fig. 7. The responses of the system excited by sine inputs

V. Conclusion

The effect of the bulk modulus on a hydraulic driven multibody system was investigated by applying different amounts of oil entrained air. The effects of the bulk modulus on the damping characteristics of a multibody system were studied by utilizing FMUs. The FMUs were built using an XML model description and the C code for

the hydraulic part. The multibody simulation was performed on real-time simulation software. The inputs to the combined system were made using Matlab-Simulink. This study aimed to demonstrate the effect of the bulk modulus on the damping behavior of multibody system dynamics employing a hydraulic circuit system.

The target was accomplished by analyzing the system with different values of the bulk modulus. The variation of the bulk modulus was achieved by manipulating the air volume fraction in the fluid. The effects of the bulk modulus on the calculation time and damping characteristics of the system were investigated. The results indicated that the air volume fraction has no significant effects on shifting the frequency response of the system. However, the study demonstrated that the pressure amplitude declines by increasing the entrained air into the oil. In addition, for some input frequencies, the damping values are higher, meaning lesser stiffness in the system. In the continuation of this work, the effects of dissolved air on the energy loss of a real-time simulation model containing a more sophisticated hydraulic system, will be investigated. Afterwards, the ultimate goal is to find a balance between the comfortability of passengers with the energy loss that it requires. This methodology can be applied to other devices as well.

Acknowledgements

The authors declare that there is no conflict of interest regarding the publication of this paper.

References

[1] A. Peiret, F. González, J. Kövecses, Multibody System Dynamics Interface Modelling for Stable Multirate Co-Simulation of Multiphysics Systems, *Mechanism and Machine Theory*, Vol. 127:52-72, 2018.

[2] M. K. Oshtorjani, A. Mikkola, and P. Jalali, Numerical Treatment of Singularity in Hydraulic Circuits Using Singular Turbation Theory, *IEEE/ASME Transactions on Mechatronics*, Vol. 24(Issue 1):144-153, 2018.

[3] J. Rahikainen, M. Kiani, J. Sopanen et al., Computationally Efficient Approach for Simulation of Multibody and Hydraulic Dynamics, *Mechanism and Machine Theory*, Vol. 130:435-446, 2018.

[4] HE Merritt, *Hydraulic Control Systems* (John Wiley & Sons, 1991).

[5] J. Watton, *Modelling, Monitoring and Diagnostic Techniques for Fluid Power Systems* (Springer Science & Business Media, 2007).

[6] BH. Cho, HW. Lee, and JS. Oh, Estimation Technique of Air Content in Automatic Transmission Fluid by Measuring Effective Bulk Modulus, *SAE Technical Paper*, 2000.

[7] Y. Jinghong, C. Zhaoneng, and L. Yuanzhang, The Variation of Oil Effective Bulk Modulus with Pressure in Hydraulic Systems, *American Society of Mechanical Engineers*, Vol. 116(Issue 1):146-150, 1994.

[8] J. Ruan, R. Burton, Bulk modulus of air content oil in a hydraulic cylinder, *ASME 2006 International Mechanical Engineering Congress and Exposition*, 2006.

[9] H. Tian, J. D. Van de Ven, Modeling and experimental studies on the absorption of entrained gas and the influence on fluid compressibility, *Journal of Fluids Engineering*, Vol. 139(Issue 10), 2017.

[10] G. Stojanoski, G. Rath, M. Gimpel, The effects of bulk modulus on the dynamics of controlled independent metering system, *16th Scandinavian International Conference on Fluid Power (SICFP19)*, 2019.

[11] S. Valilon, *Nonlinear Model and Control of Electro Hydraulic Servo-System*, Ph. D. Dissertation, Bergamo: University of Bergamo, 2017.

[12] G. Jehle, A. Fidlin, Hydrodynamic Optimized Vibration Damper, *Journal of Sound and Vibration*, Vol. 440:100-112, 2019.

[13] Y. Yin, S. Rakheja, J. Yang et al., Characterization of a Hydro-Pneumatic Suspension Strut with Gas-Oil Emulsion, *Mechanical Systems and Signal Processing*, Vol. 106:319-333, 2018.

[14] Felix, R., Bueno, Á., Modelling of a Pneumatic Actuator, (2019) *International Review of Mechanical Engineering (IREME)*, 13 (7), pp. 402-411. doi: https://doi.org/10.15866/ireme.v13i7.17219

[15] L. Kela, P. Vähäoja, Recent Studies of Adaptive Tuned Vibration Absorbers/Neutralizers, *Applied Mechanics Reviews*, Vol. 62(Issue 6):060801, 2009.

[16] CY. Lee, and CY. Chen, Experimental Application of a Vibration Absorber in Structural Vibration Reduction Using Tunable Fluid Mass Driven by Micropump, *Journal of Sound and Vibration*, Vol. 348:31-40, 2015.

[17] Y. M. Khedkar, S. Bhat, H. Adarsha, A Review of Magnetorheological Fluid Damper Technology and its Applications, *IEEE/ASME Transactions on Mechatronics*, Vol. 13(Issue 4): 256-264, 2019.

[18] M. Rahman, Z. C. Ong, S. Julai, et al., A review of advances in magnetorheological dampers: their design optimization and applications, *Journal of Zhejiang University-Science*, Vol. 18(Issue 12): 991-1010, 2017.

[19] Y. Q. Guo, Z. D. Xu, B. B. Chen, C.S. Ran, W.Y. Guo, Preparation and Experimental Study of Magnetorheological Fluids for Vibration Control, *International Journal of Acoustics and Vibration (IJAV)*, Vol. 22(Issue 2): 194-200, 2017.

[20] Mirdoraghi, S., Faridmehr, I., Md Tahir, M., Performance of Viscoelastic Dampers Under Explosive Loading in Steel Frames, (2018) *International Journal of Earthquake Engineering and Hazard Mitigation (IREHM)*, 6 (4), pp. 111-118.

[21] B. Titurus, Generalized liquid-based damping device for passive vibration control. *AIAA Journal*, Vol. 56(Issue 10): 4134-4145, 2018.

[22] U. Ferdek, J. Łuczko, Nonlinear modeling and analysis of a shock absorber with a bypass. *Journal of Theoretical and Applied Mechanics*, Vol. 56(Issue 3), 615-629, 2018.

[23] B. Geng, L. Gu, J. Liu, Novel Methods for Modeling and Online Measurement of Effective Bulk Modulus of Flowing Oil, in *IEEE Access*, Vol. 8, pp. 20805-20817, 2020.

[24] V. Popov, *Contact Mechanics and Friction [Kontaktmechanik und Reibung]* (Springer, New York 2009).

[25] MP. Paidoussis, *Fluid-Structure Interactions: Slender Structures and Axial Flow* (Academic Press, 1998).

[26] JD. Van de Ven, On Fluid Compressibility in Switch-Mode Hydraulic Circuits-Part I: Modeling and Analysis, *Journal of Dynamic Systems, Measurement, and Control*, Vol. 135(Issue 2):021013, 2013.

[27] J. Watton, *Fluid Power Systems: Modeling, Simulation, Analog and Microcomputer Control* (Prentice-Hall Hemel Hempstead, UK, 1989).

[28] P. Czop, and D. SŁawik, A High-Frequency First-Principle Model of a Shock Absorber and Servo-Hydraulic Tester, *Mechanical Systems and Signal Processing*, Vol. 25(Issue 6):1937-1955, 2011.

[29] J. Cuadrado, D. Dopico, A combined penalty and semirecursive formulation for closed-loops in MBS, *Proceedings of the Eleventh World Congress in Mechanism and Machine Science*, vols, pp. 1–5, Citeseer, 2004.

[30] A. Avello, JM. Jiménez, E. Bayo et al., A Simple and Highly Parallelizable Method for Real-Time Dynamic Simulation Based on Velocity Transformations, *Computer Methods in Applied Mechanics and Engineering*, Vol. 107(Issue 3):313-339, 1993.

[31] JG. De Jalón, E. Bayo, *Kinematic and Dynamic Simulation of Multibody Systems: The Real-Time Challenge* (Springer Science & Business Media, 2012).

[32] DS. Bae, and EJ. Haug, A Recursive Formulation for Constrained

Mechanical System Dynamics: Part II. Closed Loop Systems, Journal *of Structural Mechanics*, Vol. 15(Issue 4):481-506, 1987.
[33] J. Yao, Z. Jiao, D. Ma et al., High-Accuracy Tracking Control of Hydraulic Rotary Actuators with Modeling Uncertainties, *IEEE/ASME Transactions on Mechatronics*, Vol. 19(Issue 2):633-641, 2013.
[34] W. Borutzky, B. Barnard, and J. Thoma, An Orifice Flow Model for Laminar and Turbulent Conditions, S*imulation Modelling Practice and Theory*, Vol. 10(Issue 3-4):141-152, 2002.
[35] HM. Handroos, and MJ. Vilenius, Flexible Semi-Empirical Models for Hydraulic Flow Control Valves, *Journal of Mechanical Design*, Vol. 113(Issue 3):232-238, 1991.
[36] H. Feng, Q. Du, Y. Huang, Y. Chi, Feng, Hao, et al., Modelling study on stiffness characteristics of hydraulic cylinder under multi-factors, *Journal of Mechanical Engineering*, Vol. 63(7-8): 447-456, 2017.
[37] Frosina, E., Senatore, A., Buono, D., Monacelli, G., Pintone, F., Study of the Performance of the Hydraulic Circuit of an Agricultural Machine with a Lumped Parameter Approach, (2017) *International Review on Modelling and Simulations (IREMOS)*, 10 (1), pp. 26-36.
doi: https://doi.org/10.15866/iremos.v10i1.11213
[38] A. Peiret, J. FranciscoGonzález, M. Teichmann, Interfacing Multibody Dynamics Stepping Formulations in Co-Simulation Setups, *Proceedings of the ASME 2018 International Design Engineering Technical Conferences &Computers and Information in Engineering ConferenceIDETC/CIE* 2018 August 26-29, Qu´ebec City, Canada, 2018.
[39] Y. Q. Guo, Z. D. Xu, B. B. Chen, C.S. Ran, W.Y. Guo, Influence of coupling approximation on the numerical stability of explicit co-simulation, *Journal of Mechanical Science and Technology*, 1-10, 2020.
[40] R. Kübler, and W. Schiehlen, Modular Simulation in Multibody System Dynamics, *Multibody System Dynamics*, Vol. 4(Issue 2-3):107-127, 2000.
[41] C. Andersson, *Methods and tools for co-simulation of dynamic systems with the functional mock-up interface*, Ph.D. dissertation, Lund Univ., 2016.
[42] C. Gomes, B. Legat, RM. Jungers et al., Stable adaptive co-simulation: a switched systems approach, *IUTAM Symposium on Co-Simulation and Solver Coupling*, 2019.
[43] T. Blochwitz, *Functional Mock-Up Interface for Model Exchange and Co-Simulation*, 2014 July [Online], Accessed January 2016. https://Www. Fmi-Standard.Org/Downloads
[44] L. I. Hatledal, A. Styve, G. Hovland and H. Zhang, A Language and Platform Independent Co-Simulation Framework Based on the Functional Mock-Up Interface, in *IEEE Access*, Vol. 7: 109328-109339, 2019.
[45] Modelica Association, *Modelica Language Specification Version* 3.4 (2017).
[46] IEEE Standards Association, *IEEE Standard for Modeling and Simulation(M&S) High Level Architecture (HLA)* (2012).

Authors' information

Lappeenranta-Lahti University of Technology (LUT University), Lappeenranta 53850, Finland.

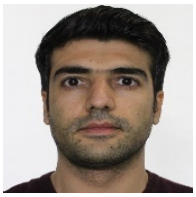

Manouchehr Mohammadi is born in Persia. He received the B. Sc. From QIAU, Persia in 2009, and M. Sc degrees in department of Mechanical engineering, from Lappeenranta-Lahti University of Technology (LUT), Finland in 2017. He is currently a junior researcher at the Lappeenranta-Lahti University of Technology. His current research interest includes designing of real-time simulation models.
E-mail: Manouchehr.mohammadi@lut.fi

Mehran Kiani-Oshtorjani is a doctoral student at Lappeenranta University of Technology since 2016. His scientific research areas include hydraulic systems, dynamic and thermal behavior of granular materials, multi-phase flows, and computational fluid dynamics (CFD). He is an expert in real-time simulations, both as an algorithm designer and professional scientific programmer
E-mail: Mehran.kiani@lut.fi

Aki Mikkola received the Ph. D. degree in machine design, in 1997. Since 2002, he has been working as a Professor at the Department of Mechanical Engineering, Lahti-Lappeenranta University of Technology, Lappeenranta, Finland. He is currently leading the research team of the Laboratory of Machine Design, Lahti-Lappeenranta University of Technology. His research interests include machine dynamics and vibration, multibody system dynamics, and bio-mechanics. He has been awarded five patents and his contributed to more than 90 peer-reviewed journal articles.
E-mail: Aki.Mikkola@lut.fi

